# Simulation of Virtual Nanoparticle tracking using calculated forces for an Atomic Force Microscope and Optical Tweezers

Shailakash Kode*, Suren N. Dwivedi**, Pavel G. Ikonomov***

*Department of Mechanical Engineering, sxk9036@louisiana.edu
**Department of Mechanical Engineering, dwivedi@louisiana.edu
***Department of Industrial and Manufacturing Engineering, pavel.ikonomov@wmich.edu

## ABSTRACT

Nanomanufacturing necessitates manipulation of nanoparticles in order to build functional three-dimensional structures. Manipulation of nanoparticles takes place in microenvironments where it is not practical for the user to manually interact with the nanoparticles. So far, there is not a standard device that has been used to manufacture products at nanoscale. In order to achieve effectiveness and reliability in the field of nanomanufacturing and nanoassembly, it is necessary to study the forces exerted on nanoparticles, the interaction between the manipulation devices, and the substrate on which the particles are present. In this situation, Virtual Reality (VR) techniques not only help guide these manipulations, but also allow the user to be virtually present in these microenvironments. This paper proposes a VR technique to track the movement of the nanoparticles during the interaction with an atomic force microscope and optical tweezers using simulated forces. The forces considered during the process include both contact and non-contact forces experienced by the nanoparticles. Using the standard equations, these forces were calculated in MatLab and provided as input to the VR software (Eon Reality) to represent the direction of particle movement. Visualization and control of nanoparticle movement is demonstrated by varying the force inputs. Once optimized, this approach can be used to control the nanoparticle movement and assemble these particles in an actual nanomanufacturing system.

***Keywords***: Virtual Reality, nanoparticles, nanoassembly, AFM, Optical Tweezers

## 1. INTRODUCTION

Nanotechnology is the field of science, which enables us to understand, control, and work with systems at the atomic, molecular level to create devices and use materials with fundamentally new molecular organization [1, 22]. "Nanomanipulation" refers to particles in the size range of a few nanometers being pushed, oriented, positioned, bent, and twisted by varying certain parameters, usually external force, of a probe [2]. By precise control of atoms, molecules, and nanoscale level objects, it is possible to construct drug delivery systems, monitor protein functions in living cells in real time [3], and fabricate terabyte capacity memory chips, integrated sensors, and other communication tools for novel applications. Manufacturing products at nanoscale level is experiencing many limitations due to lack of availability of standard tools to manipulate nanoparticles. Different devices have been used to manipulate and control particle size, ranging from a few micrometers to a few nanometers. The Atomic Force Microscope (AFM) has been widely used [4, 11] to provide an image of the scanned surface and understand dynamic modeling procedures. The AFM resolution in the x-y plane ranges from 0.1nm to 1nm and up to 0.01 nm in z direction [5, 6]. The simple AFM does, however, have certain limitations. For example, it cannot perform complex three-dimensional tasks such as pick and place operations, and the accountability of forces in the third direction is limited and there are chances of nanoparticle sticking to the probe [2].Nanoparticles experience different contact and non-contact forces using the AFM during the manipulation process. It is, therefore, crucial to model the interaction of these forces interaction with the manipulating probes. So far, there is not a standard device that has been used to manufacture products at nanoscale. In order to achieve effectiveness and reliability in the field of nanomanufacturing and nanoassembly, it is necessary to study the forces exerted on nanoparticles, interaction between the manipulation devices, and the substrate on which the particles are present. The present challenges in nanotechnology are to achieve control (ability to manipulate), to consider various processing methods, and to build functional three-dimensional structures (3-D) structures. The construction of 3-D structures using pick and place operations is still in the nascent stages of development, and the literature available with respect to their representation and control is limited. To conveniently manipulate the particle in 3-D space, a new technique called Optical tweezers is being explored to manipulate nanoparticles by mere radiation pressure of light without any mechanical contact. In this paper, forces experienced by the nanoparticle during interaction with AFM and optical tweezers are presented. The forces considered to contribute significantly to the nanoparticle motion while interacting with AFM are classified as contact and non-contact forces. The sum of Vander Waals, gravitational and electrostatic forces represents the non-contact forces and the sum of capillary and frictional forces represents the contact forces. Treatment of the particle using optical tweezers technique depends on size of the particle measured in terms of wavelength of the laser. Modeling of

forces using Ray optics regime, where diameter of the particle is greater than wavelength of the laser beam and by using Rayleigh regime in which the diameter of the particle is less than the wavelength of the laser beam.

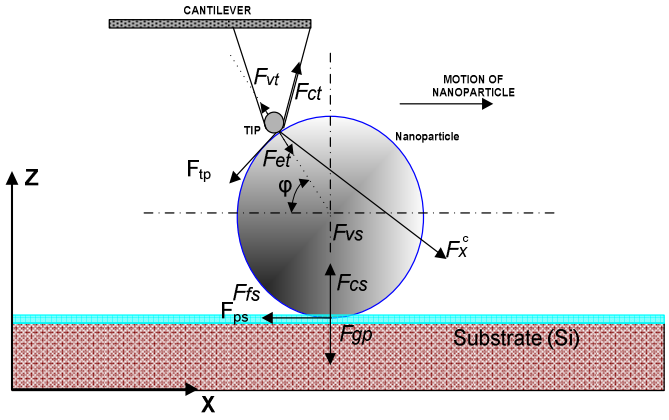


Figure 1: Schematic representation of forces

The dynamic behavior of the particles [12, 13] due to different interaction forces between the particle-particle, particles-substrate, and probe-particle must be addressed. Manipulation of nanoparticles takes place in microenvironments where the user usually cannot see and interact with the particle manually. In this situation, Virtual Reality (VR) not only comes to our aid to help guide these manipulations, but also allows the user to feel immersed in these microenvironments. In this work, various contact and non-contact forces experienced by the different particles with different properties during manipulation process have been modeled for AFM and Optical tweezers. The values of different forces that contribute significantly to determine the motion of the particle are given as input to the VR system. The magnitudes of different contact and non-contact forces were calculated using MATLAB and were provided as input to the VR software (EON Reality) to simulate the process and particles motion are controlled and tracked.

## 2. SIMULATION OF FORCES

The precision of representation of nanoparticle movement depends on various dominant forces and their magnitudes in a given situation. In this paper, for interaction of the particle with an AFM, the forces considered are Vander Waals force, capillary force, electrostatic force, frictional force and gravitational force. For interaction of the particle with laser beam (optical tweezers), scattering force, gradient force and total force as their magnitude is considered. Using the AFM for handling micro and nanoscale samples, forces that contribute significantly to the movement of the particle are categorized as contact and non-contact forces [9]. The sum of Vander Waals force, electrostatic force, and gravitational force constitute the total non-contact forces while interacting with AFM. Capillary and friction forces together constitute the contact forces. Contact and non-contact forces together potentially affect the direction of nanoparticle motion. Further, it is assumed that the cantilever tip in contact passes through the particle after touching it [13], the acting vector $F_x$ has force acting against the sum of both the contact and non-contact forces. It is assumed that whenever the tip approaches the particle, the particle does not stick to it and the force ($F_{ps} \geq F_{tp} \cos\varphi$) required to push the particle is sufficient to move the particle and not break the tip. $F_{ps}$ is the adhesive force and $F_{tp}$ is the force between the tip and the particle, and φ is the contact angle between the particle and the tip. A schematic representation of these forces is shown in the Figure 1. The particle is put in motion by the cantilever driving force. Motion of the particle depends on the magnitude and direction of the driving force, the point of contact of the tip of the cantilever with the particle, and the total sum of contact and non-contact forces experienced by the particle.

### 2.1 AFM Interaction with Particle and Substrate

Vander Waals forces are weak intermolecular forces, which exist in all environments for all the materials in contact. Vander Waals forces depend on particle geometry, material type, and distance between the particles [13]. Vander Waals forces were assumed to be present between particle-tip ($F_{vdw\_tp}$) and particle-substrate ($F_{vdw\_ps}$). Under the assumption that both the tip of the cantilever and the particle are spherical and according to continuum mechanics, the solution can be represented by the equation (1) for Vander Waals' forces between the tip and the particle and equation (2) between the particle and the substrate[13, 14].

$$F_{vdw\_tp} = \frac{H(h+r_{plus})}{3}\left\{\frac{2R_pR_t}{h^2(h+2r_{plus})^2} + \frac{2R_pR_t}{((h+2r_{plus})^2 - r_{minus}^2)^2} + \frac{1}{h(h+2r_{plus})} - \frac{1}{(h+r_{plus})^2 - r_{plus}^2}\right\} \quad (1)$$

$$F_{vdw\_ps} = -\frac{H}{6}\left\{\frac{R_p}{h^2} + \frac{R_p}{(h+2R_p)^2} - \frac{1}{h} + \ln\frac{1}{(h+2R_p)}\right\}. \quad (2)$$

Here, $r_{plus} = R_t + R_p$ and $r_{minus} = R_t - R_p$ where $R_p$ is the radius of the particle (m), $R_t$ is the radius of the tip (m), $H$ is the Hamacker constant whose range is ($0.4 \times 10^{-19}$J < $H$ < $5 \times 10^{-19}$ J) for all materials and h is tip-particle surface distance (m). Under ambient conditions, there is always a water layer on the surface of the probe and on the substrate due to presence of moisture in the air. If the variation of the meniscus height around an irregular contact is small, the capillary force due to the variation in the meniscus height is given by the expression [14, 16]

$$F_{cap} = \frac{4\pi R_t \gamma \cos\theta}{1+\frac{D}{d}} \qquad (3)$$

Where $\gamma$ is the surface tension of water in N/m, $\theta$ is the angle of contact between the tip and the water vapor interface, $D$ is the distance between the tip and the substrate, and $d$ is the distance the tip extends into the layer present on the surface of the particle. When a particle is pushed against the surface of the substrate, friction forces play a significant role in contributing to the overall resultant force in the environment. The friction over the surfaces due to tip-particle interaction and particle-substrate interaction is calculated. In the present context, gravitational forces, though small, were calculated using Newton's second law of motion. If the particle is an insulator, there are charges trapped on the perimeter of the particle, and when it is pushed by the AFM tip, the charges surrounding perimeter of the particles are transferred to the AFM tip due to contact electrification and triboelectrification. Electrostatic force between the particle and tip can be approximated as [13, 14]

$$F_{el} = -\left(\frac{(\varepsilon_0 U_{as}^2 S}{2h^2}\right) \qquad (4)$$

Where $\varepsilon_0$ is the permittivity (F/m), $U_{as} = (\varphi 1 - \varphi 2)/e$ is the voltage difference (V), $\varphi 1$ & $\varphi 2$ are the work functions of the two surfaces, $e = 1.602 \times 10^{-19}$ C is the charge of an electron, $S = 4\pi R_t r$ is the Shared contact area (Sq-m), and h is the distance between the tip and the particle (m).

## 2.2 Optical Tweezers Interaction with the Particle

In an effort to achieve the goal of convenient three-dimensional manipulation of sub-microscopic particles by a non-contact method, optical tweezers technique is being explored as a powerful tool in the field of nanotechnology. In 1970, Arthur Ashkin, first demonstrated that particles can be accelerated and trapped by mere radiation pressure of a light [17] instead of using a mechanical means to manipulate an object. Optical tweezers, known as optical traps, hold dielectric particles in the size range of µm to nm. Optical tweezers, as non-contact type manipulators, are able to apply loads in the order of pico-Newton (of the order $10^{-12}$ Newton), which may be applied with sub-pN resolution on objects whose characteristic dimensions are similar to the wavelength [19] of a laser. When a tightly focused laser beam is passed through the microscope objective with high numerical aperture, momentum of light is imparted to a particle under the beam, and the particle behaves as a dipole and is drawn towards the point of highest intensity [20-24].

The beam is focused on the narrowest point of a microscope objective of high numerical aperture, which is called the beam waist, containing a strong electric field. At the center of the beam, the dielectric particles are attracted along the gradient, which represents a strong electric field. The force acting on the dielectric particle, when treated as a point dipole, is proportional to the gradient along the intensity of the beam, and this force is termed the gradient force. In other words, the gradient force described here tends to attract the particle to the region of highest intensity. This results in a force pushing the particle slightly downstream from the exact position of the beam waist, and this fore is known as the scattering force. The scattering force depends linearly on the intensity of the beam, the cross section of the particle and the index of refraction of the trapping medium. In the Figure 2, arrow lengths are proportional to the magnitude of the forces. The size of the particle being trapped plays an important role in nanomanipulation purposes to calculate the exerted optical forces using Optical tweezers. In case of spherical particles, if diameter of the particle is greater than the wavelength of the laser, the ray optics approach is used [21]. If the wavelength of the laser is less than the dimensions of the particle, Rayleigh Approximation (RA) is used. In the Rayleigh regime, the particle is treated as a dipole, and electromagnetic equations are used in computing the forces [23-26]. Most of the optical tweezers use $TEM_{00}$ mode Gaussian beams. Gaussian beam is an electromagnetic radiation whose transverse electric field and irradiance is described by Gaussian functions.

### 2.2.1 Ray Optics Approach

Ray optics approach was used to calculate the forces on micron sized particles [17, 20, 21]. Trapping of these particles is conducted by geometric approach in which the incoming laser impinging on the particles is assumed to consist of a number of rays, each with the appropriate intensity and propagated in straight lines [17]. Each ray has a characteristic of a plane wave and changes its direction when it refracts, reflects, and changes polarization at dielectric interfaces according to Fresnel's formulas. The difference in momentum will apply a force on the object due to conservation of momentum, and the total force from which the particle is trapped is a result of the sum of contributions made from all the rays. The Ray optics approach uses Snell's Law and Fresnel's formulas and does not take into account different sphere sizes because the phase front of the incident wave is assumed not to change its shape at the focal point [17].

Gradient force ($F_g$) tends to move towards the center of the beam where there is highest intensity of light, and scattering force ($F_s$) moves away from the center of the beam. In order to achieve a stable trap, it is necessary for $F_g > F_s$. Forces acting on the particle depend entirely on the dimensionless factor 'Q,' which is the called the Trapping Efficiency. 'Q' depends on R, T, angle of incidence, and angle of refraction. The net force at the center of the sphere is divided into two components [18]: gradient force and

scattering force. Gradient component acting along the gradient of the beam pointing along the intensity gradient of light is called the gradient force (Equation5) and force component pointing in the direction of incident light is called the scattering force [18, 28] (Equation 6).

$$F_g = \frac{nP}{c}\left\{R\sin 2\theta - \frac{T^2[\sin(2\theta-2\varphi)+R\sin 2\varphi]}{1+R^2+2R\cos 2\varphi}\right\} \quad (5)$$

$$F_s = \frac{nP}{c}\left\{1+R\cos 2\theta - \frac{T^2[\cos(2\theta-2\varphi)+R\cos 2\theta]}{1+R^2+2R\cos 2\varphi}\right\} \quad (6)$$

where $R=\left(\frac{n1-n2}{n1+n2}\right)^2$ is the Fresnel's reflection coefficient and $T=1-R.$ is the .Fresnel's transmission coefficient

### 2.2.2 Rayleigh Approximation

During the Rayleigh approximation, the particles having dimensions less than the wavelength of the laser are considered. The electromagnetic field polarizes the particles and orients the charges in the direction of the field, and the gradient of the electromagnetic field applies force on the particle [26]. The force on the dipole divides itself naturally into two components: scattering force component pointing in the direction of incident light and gradient force component pointing in the direction of the intensity gradient of the light [18, 26, 27]. Trapping of the particles in the Rayleigh regime can be done using a weakly focused and a tightly focused Gaussian beam. The concept of weak focused and tightly focused beams depends on the beam waist, $w_0$, as a multiple of the wavelength of the laser beam. Two scenarios are taken into consideration in Rayleigh approximation. One having beam waist greater than or equal to 10 λ and the second scenario having beam waist less than or equal to 8 λ (where λ is the wavelength of the laser). Considering $w_0$ = 10λ as a Gaussian beam that is not too tightly focused and one which has a waist radii not much smaller than the wavelength (**λ**), paraxial approximation holds good. Gradient force [29] along the z-direction in the Cartesian coordinate system along the axis of the beam impinging the particle is given by equation (7) where $\hat{z}$-unit vector, $P=(\pi w_0 n_2 \varepsilon_0 c E_0^2)/4$ is the laser beam power (Watt), $E_0$ is the amplitude of intensity (V/m), $n_2$ is the refractive index of the surrounding media, and $(\tilde{x},\tilde{y},\tilde{z})=(x/w_0, y/w_0, z/kw_0^2)$ represents the normalized spatial coordinates [29]. Considering the beam waist to be less than or equal to 8λ as a tightly focused Gaussian beam where the waist radii is not much larger than the wavelength of the laser, paraxial approximation

$$F_{grad,z(r)} = -\hat{z}\frac{2\pi n_2 a^3}{c}\left(\frac{m^2-1}{m^2+2}\right)\left(\frac{8\hat{z}/(kw_0)^2}{1+(2\hat{z})^2}\right)\left[1-\frac{2(\tilde{x}^2+\tilde{y}^2)}{1+(2\hat{z})^2}\right]\left(2P/\pi w_0^2\right)$$

$$X\frac{1}{1+(2\hat{z})^2}\exp\left[-\frac{2(\tilde{x}^2+\tilde{y}^2)}{1+(2\hat{z})^2}\right] \quad (7)$$

and first order correction does not hold good to achieve a stable trapping of particles. Another simple yet effective approach is to use a fifth-order corrected Gaussian beam, which is very much valid for tight to weakly focused beams [25, 26].

$$Q_{scat,z} = \frac{16}{27}\frac{\alpha^2}{w_0^2}\left(\frac{2\pi n_2}{\lambda}\right)^4 a^6\left[\frac{1}{1+(2\tilde{z})^2}\right] \quad (8)$$

$$Q_{grad,z} = -\frac{32\alpha}{w_0^4}\left(\frac{\lambda}{2\pi n_2}\right)a^3\tilde{z}\left[\frac{1}{1+(2\tilde{z})^2}\right]^2 \quad (9)$$

where $\tilde{z}=(z/w_0^2)(\lambda/2\pi n_2)$ is the normalized spatial coordinate in the axial direction, $\alpha=3(m^2-1/m^2+2)$ is polarization from Clausius-Mosotti relation , $m=n1/n2$ is the relative refractive index, $a$ is the radius of the particle (m), and $w_0$ is the beam waist (m). To calculate the point

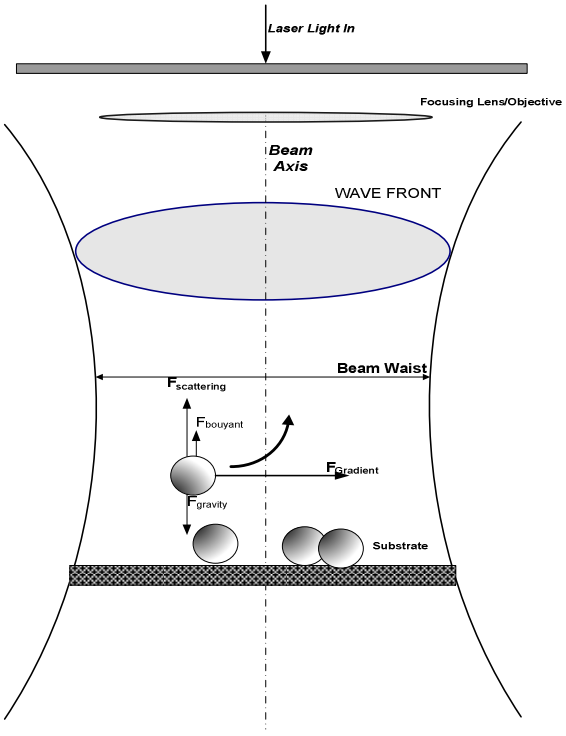


Figure 2: Forces exerted on a particle during interaction with a laser beam

with maximum axial trapping efficiency, we need to calculate the value of "z" and for that purpose we take the first derivative of Equation (10). This value of z could be either extreme minima or extreme maxima. For the value to be at maxima, the second derivative must be greater than or equal to zero.

$$Q_{total} = Q_{scat,z} + Q_{grad,z} \qquad (10)$$

$$\frac{dQ_{total,z}}{dz} = 0 \qquad (11)$$

## 3. RESULTS AND DISCUSSION

### 3.1 Interaction with an AFM

Vander Waals forces are considered for different tip materials on a silica substrate. Vander Waals forces between tip and particle are shown in Figure 3calculated using Equation 1. In Figure 4, forces for particles and the substrate for different tip materials of the AFM, and were plotted against changes in the distances between the tip and the particle calculated using Equation 2. It was observed similar pattern of forces without much deviation along either axis. From Figure 4, it can be noted that between 2nm and 4nm particle and tip distance for iron oxide, mica, and silica tips, the Vander Waals force is almost negligible whereas the values of forces of for gold and silver tips posses reasonable values. It can be observed that Vander Waals forces for different particles on a silica substrate follow the same pattern in a different direction depending on the point of contact. Attractive forces (negative) become almost negligible when the distance of separation between the particle and substrate is greater than 9nm for iron oxide, paraffin wax and mica particles. Gold and silver particles attractive forces become almost negligible when the distance between the particle and substrate is greater than 11nm.

Capillary forces were calculated for a pair of three tips and substrate using the Equation 3 shown in Figure 5. Capillary forces have been calculated for gold, polymer, and paraffin wax coated tips. Gold coated tips were expected to make contact angles of $0^0$, and paraffin wax and polymer coated tips were expected to make contact angles between $100^0$ and $110^0$, indicating the wetting characteristics [14, 16]. From Figure 5, it can be observed that repulsive and attractive forces decreased as the distance between the coated tip and the substrates was increased [16], and it reached a negligible value after 11nm. Electrostatic forces between the tip and particle are calculated using Equation 4. Considering the semi-conducting silica substrate, the electrostatic forces arise due to local charging or charge trapping, which occurs when the particle moves with respect to the tip. This force usually depends on the material selected for the tip[15]. From Figure 6, it can be observed that when the distance between particle and tip is greater than 4nm, electrostatic forces between the particle and tip are almost negligible.

### 3.2 Interaction with Optical Tweezers

In this paper, forces experienced by the nanoparticle during manipulation using Optical tweezers technique are also studied. Figure 7 shows radiation forces for a dielectric sphere when impinged by a ray at different angles using ray optics approach. $F_s$, $F_g$, and $F_{mag}$ represent the scattering force, gradient force, and magnitude respectively from Equations 5 and 6.

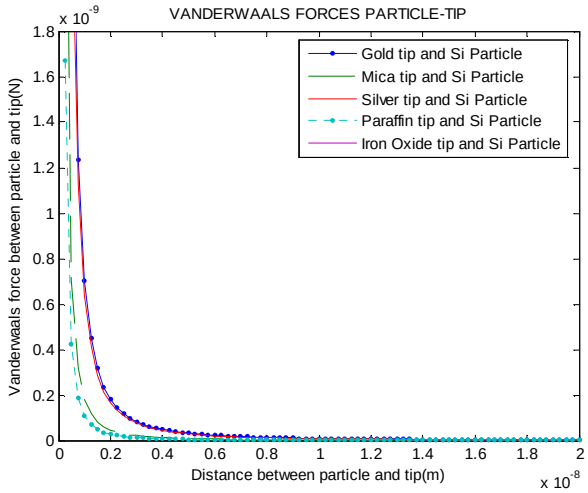


Figure 3: Vander Waals forces between tip and particle

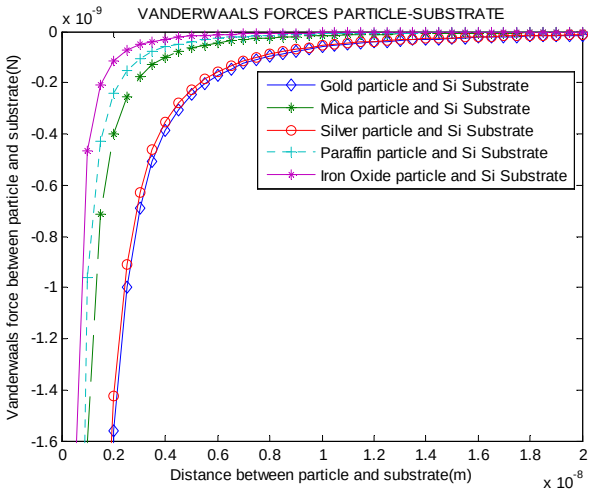


Figure 4: Vander Waals forces between particle and substrate

The results shown are in agreement with experimental results [19]. Trapping efficiencies were found to increase were up to 52 degrees (angle of incidence) and decrease after that and radiation forces also showed the same pattern due to direct proportionality on the values of trapping efficiencies.

Figure 7 presents the correctness of expression for radiation force, derived in[18], along the transverse component located on the plane of the beam waist for a polystyrene sphere as a function of transverse position. Results shown in Figure 8 are for a slightly divergent beam impinging on a polystyrene sphere in water with relative index of refraction of 1.2 with wavelength 0.5145 µm for sphere sizes 5nm, 10nm, 50nm, and 100 nm. Calculation of radiation force is carried out using Equation 7.The particle is trapped near the

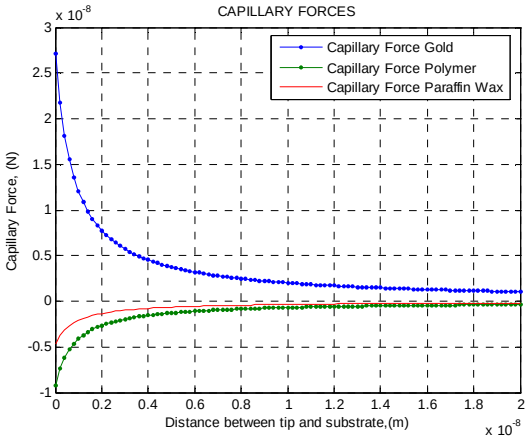


Figure 5: Capillary forces for different coating on tips and Si substrate

center of the beam and from Figure 9 for a 5nm size dielectric particle, the radiation force exerted is ±5 X $10^{-9}$ pN on either side of the center of the beam waist. In order to achieve a stable trap, it is necessary for the beam to be not a diverging one and should be a tight or reasonable tight as explained. Figure 9 shows the results obtained by a using fifth-ordered approximation of Gaussian beam having trapping forces for dielectric particles with a diameter, which is less than or equal to the wavelength of the laser in arbitrary electromagnetic fields. Positive values for trapping efficiency indicate forces pushing the particle in the direction of propagation of the beam and the negative trapping efficiencies indicate the particle being pulled in the opposite direction of propagation of the beam. For a reasonably tight beam [24, 25], where beam waist is equal to eight times the wavelength of the laser, the scattering force efficiency, gradient force efficiency, and total axial trapping efficiency for a particle of radius 100nm with refractive index 1.57 and a wavelength of 1.064 µm suspended in an aqueous medium (n=1.33). Trapping efficiencies were calculated using equation 8 and 9. It was found that the particle was being trapped at 8.8 X $10^{-6}$m which is near the minima of the curve and is the region of interest. The negative trapping efficiency indicates that the particle is being pulled towards the beam i.e. in a direction opposite to its propagation and this is termed as backward trapping efficiency. The results shown in Figure 10 provide the values of backward trapping efficiencies for spheres of size varying from 25nm to 500nm. Backward trapping efficiencies are calculated using Equations 7, 8 and 10s for a laser power of 0.1W for radius of the sphere up to 500 nm and the corresponding forces shown are in the range of pico-Newton.

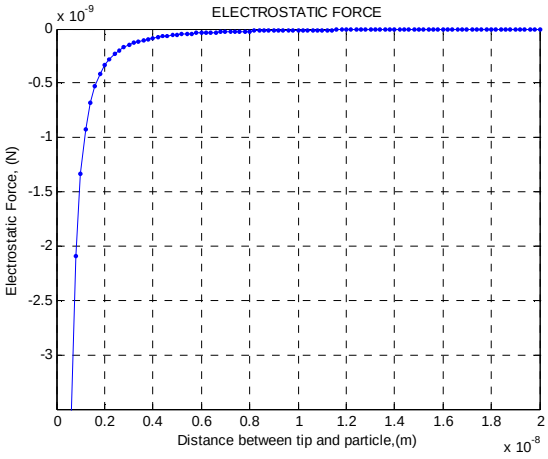


Figure 6: Electrostatic forces between tip and particle

## 3.3 Virtual Reality Simulations

### 3.3.1. Virtual Reality Simulation of the Particle Interaction with AFM

Simulation environment is modeled in EON Reality software. During the run time, different values of the forces calculated using the MATLAB programs are provided as input to the simulation environment in the VR interface, Figure 11. After various force inputs are provided to the VR system interface, the motion is induced at the cantilever tip by providing a required driving force as an input value. Depending on the motion, direction, and interaction between the particle and cantilever, additional forces may influence the motion of the particle. Forces between substrate and particles are frictional forces, gravitational force and capillary forces. Forces between tip and particles are Vander Waals Forces, capillary forces, and electrostatic forces.

### 3.3.2 Virtual Reality Simulation of the Particle Interacting with the Laser

Nanoparticle interaction with the Optical tweezers is shown in Figures 12. When the particle interacts with the laser, the radiation force is divided into two components, namely scattering force and gradient force. The forces that are given as inputs to this scenario of nanomanipulation are the scattering force, the gradient force, and the total force. It is assumed that the laser beam passes through the particle. Simulation shown in Figure 12 is for particle sizes smaller than the wavelength of the laser is being trapped and can be held in three-dimensional space. When the probe is not active, in other words, when the laser power is turned off,

the particle falls on the substrate under the influence of gravity.

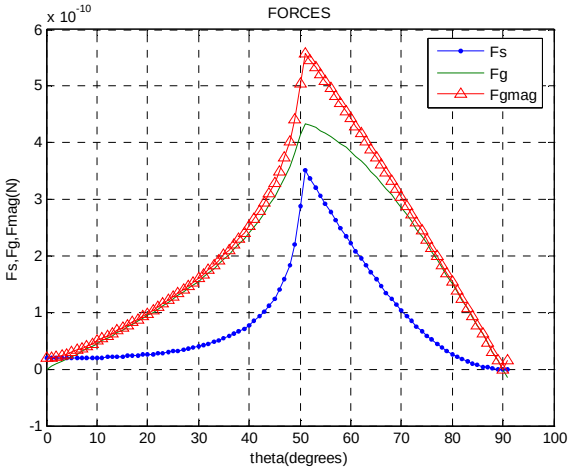


Figure 7: Forces at different angles for n=1.2 using Ray optics Approach

## 4. SUMMARY AND CONCLUSIONS

In this paper, a Virtual Reality tool is presented to manipulate nanoparticles in three- dimensional space by providing the values of different forces during the interaction of the probe with the particle. Different contact forces and non-contact forces in case of AFM interaction with the nanoparticle are shown in this simulation. The forces were calculated in MATLAB. It is also shown that the resultant interaction among the tip, particle, and substrate generates momentum in a direction predicted by the VR simulation and moves the particles in three-dimensional space. This controlled tracking and manipulation of nanoparticles will pave the way for nanoassembly in a virtual environment. Forces considered during the interaction of the particle using Optical tweezers were scattering force, gradient force, and the total optical force exerted on the particle. This VR system can not only visualize the geometry of the nanoparticle, probe (AFM tip plus Optical tweezers) and the substrate, but can also give the user an idea of the acting force vectors during the nanomanipulation process. One of the interesting features of this simulation is, during the run-time, different force vectors are shown as they become active. For instance, friction forces between the tip-particle and particle-substrate cannot be seen as active in the VR system until the tip starts to interact with the particle on a substrate. Simulation of nanomanipulation depends on the physical and chemical properties of the particle, laser power, distance between the particle and the tip and more importantly, on the size of the particle. This system eliminates the uncertainties of determination of position and direction of nanoparticle. In other words, this VR system is not just a tool to move the nanoparticles in three-dimensional space but it can also serve as a tool to track, control, and manipulate the particles for nanoassembly and nanomanufacturing by using the forces along with their magnitude and direction.

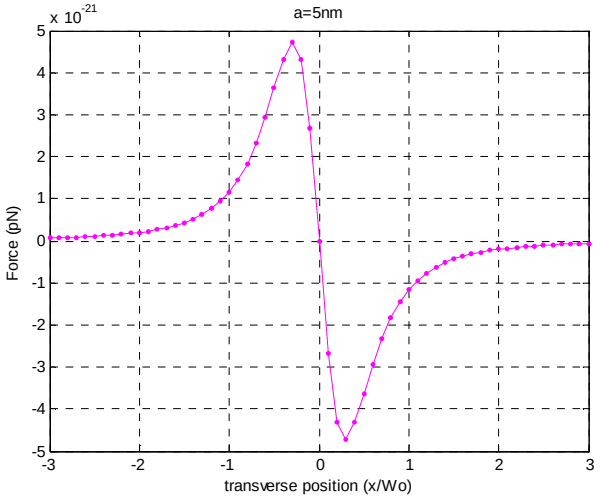


Figure 8: Optical trapping forces on a dielectric sphere of radius 5nm

In this study, the VR model not only provides the user to work on single nanoparticles but also allows simulation of assembly of nanoparticles particles to provide meaningful three-dimensional structures and eventually pave the way for nanomanufacturing. Once the real particles are assembled using the available manipulation devices, we can observe the relative positions and provide feedback to the VR model. Forces between the probe (cantilever tip, Optical tweezers), particles, and substrate can be represented using the models described in the methodology section. This model can be optimized to develop a feedback system from the actual manipulation system to the VR system. Once optimized, this model can be used to automate the process of nanoassembly. The technique used in this VR simulation model can be further explored in other virtual environments like CAVE Virtual Environments.

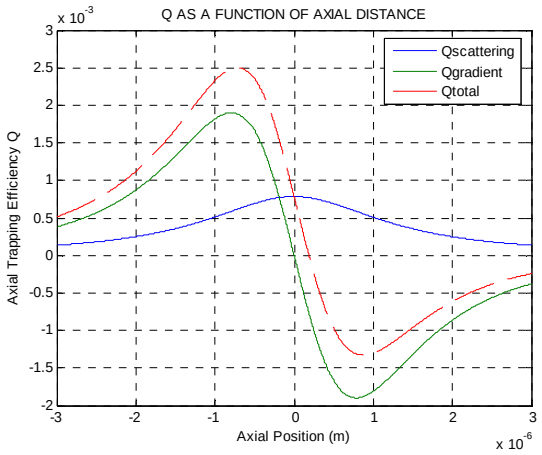


Figure 9: Axial trapping efficiency as a function of axial position

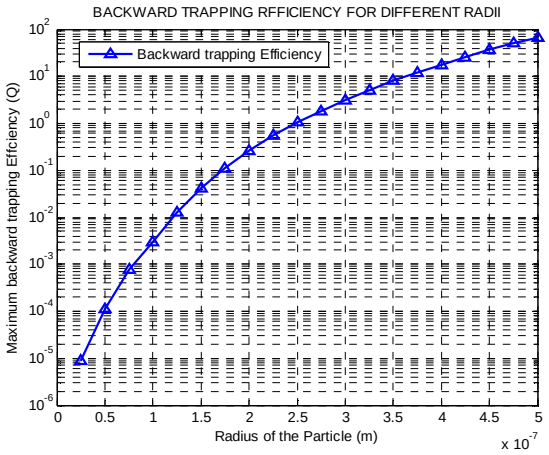


Figure 10: Maximum backward trapping efficiency for varying sphere radii

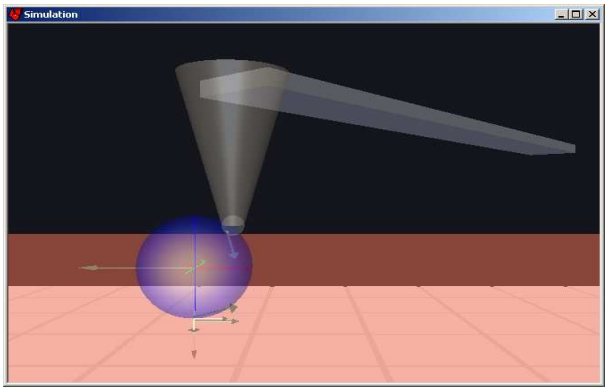


Figure 11: VR Simulation of the interaction forces using AFM

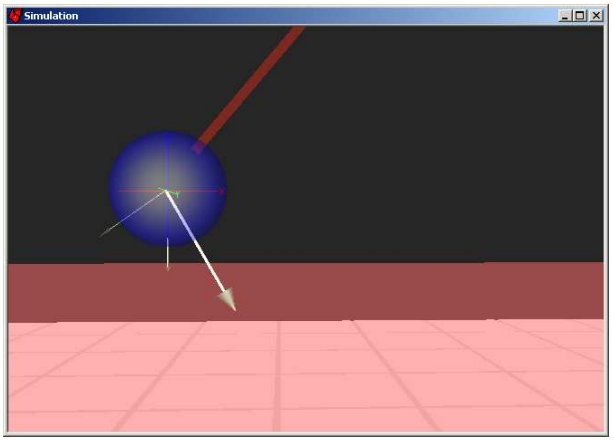


Figure 12: VR Simulation of the interaction forces using Optical tweezers

## 5. REFERENCES


[1] National Nanotechnology Initiative (NIN), http://www.nano.gov/html/facts/whatIsNano.html

[2] Sharma, G., Mavroidis, C., and Ferriera, A., 2005, *Virtual Reality and Haptics in Nano- and Bionanotechnology*, Handbook of Theoretical and Computational Nanotechnology, American Scientific Publishers, Chap.40, pp. 1-33.

[3] Tang, Q., Zhang, Y., Chen, L., and Wang, R., 2005, "Protein delivery with Nanoscale precision," *Nanotechnology Conference and Trade Show*, 16, pp. 1062-1068.

[4] Sitti, M., and Hashimoto, H., 2000, "Controlled Pushing of Nanoparticles: Modeling and Experiments," *IEEE/ASME Transactions on Mechatronics*, 5(2), pp.199-211.

[5] Binnig, G., Rohrer, H., Gerber, Ch., and Weibel, E., 1982, "7X7 Reconstruction on Si (111) in Real Space," Physical Review Letters, 50(2), pp. 122-123.

[6] Binnnig, G., Quate, C. F., and Gerber, C., 1986, "Atomic Force Microscope," Physical Review Letters, 56(9), pp. 930-933.

[7] Baselt, D., Ph.D. thesis, http://stm2.nrl.navy.mil/how-afm/how-afm.html.

[8] Tafozzoli, A., and Sitti, M., 2004, "Dynamic Modes of Nanoparticle Motion During Nanoprobe-based Manipulation," *Proc. of 4th IEEE Conference in Nanotechnology*, Munich, Germany.

[9] Requicha, A. A. G., 1999, "Nanorobotics," in Handbook of Industrial Robotics, S. Nof., Ed., John Wiley & Sons, New York, 2nd Ed.

[10] Requicha, A. A. G., 2003, "Nanorobots, NEMS, and nanoassembly," *Proc. of IEEE*, Special Issue on Nanoelectronics and Nanoprocessing, 91(11), pp.1922-1933.

[11] Garcia-Santamaria, F., Miyazaki, H. T., Urquia, A., Ibisate, M., Belmonte, M., Shinya, N., Meseguer, F., Lopez, C., 2002, "Nanorobotic manipulation of microspheres for on-chip diamond architectures," *Advanced Materials*, 14(16), pp. 1144- 1147

[12] Tafozzoli, A., and Sitti, M., 2004, "Dynamic Modes of Nanoparticle Motion During Nanoprobe-based Manipulation," *Proc. of 4th IEEE Conf. in Nanotechnology*, Munich, Germany, 1, pp. 37-40

[13] Sitti, M., Ph.D. thesis, 1999, "Teleoperated 2-D Micro/Nanomanipulation Using Atomic Force Microscope," University of Tokyo, Japan.

[14] Ikonomov, P.G., and Ghantasala, M. K., 2006, "Virtual Reality approach for nanoparticles tracking using simulated forces," *Proc. Nanotechnology Conference and Trade Show,"* 1, pp. 693-696

[15] Israelachvili, J. N., 1992, Intermolecular and Surface Forces, London, U.K., Academic Press.

[16] Eastman, T., and Zhu, D., 1996, "Adhesion Forces between Surface-Modified AFM tips and a Mica

Surface," J. American Chemical Society, 12, pp. 2859-2862.
[17] Ashkin, A., 1970, "Acceleration and trapping of particles by radiation pressure," Physics Review Letters, 24(4), pp.156-159.
[18] Prasad, P.N., 2003, *Introduction to Biophotonics*, John Wiley & Sons Inc., USA. Chap. 14.
[19] Ashkin, A., 1992, "Forces of a single-beam gradient laser trap on a dielectric sphere in the ray optics regime," J. Biophysics, Biophysical Society, 61, pp.569-582.
[20] Optical Tweezers: Theory and Current Applications http://www.iscpubs.com/articles/al/a0111bro.pdf
[21] Ashkin, A., 1997, "Optical trapping and manipulation of neutral particles using lasers," Proc. Natl. Acad. Sci., 94, pp.4853–4860
[22] Drexler, K. E., 2006, "Toward Integrated Nanosystems: Fundamental Issues in Design and Modeling," J. Computational and Theoretical Nanoscience, 3, pp.1-10.
[23] Strausser, Y. E., Heaton, M. G., 1991, "Scanning Probe Microscopy and Recent Innovations," J. American Laboratory, 26(6), pp. 20-22.
[24] Stelzer, E. H. K., and Rohrbach, A., 2001, "Optical trapping of dielectric particles in arbitrary fields," J. Optical Society of America, 18(4), pp. 839-853.
[25] Zemanek, P., Liska, M., Jonas, A., and Sramek, L., 1999, "Optical trapping of nanoparticles and microparticles by a gaussian standing wave," Optics Letters, 24(21), pp.1448-1450.
[26] Zemanek, P., Liska, M., Jonas, A., and Sramek, L., 1998, "Optical trapping of Rayleigh particles using gaussian standing wave," Optics Communications, 151, pp. 273-285.
[27] Alda, J., 2003, "Laser and Gaussian Beam Propagation and Transformation," Encyclopedia of Optical Engineering, pp. 999-1013.
[28] Ulanowski, Z., Optical Tweezers Principles and Applications," 2001, Proc. Royal Microscopy Society, 36, pp. 7-14.
[29] Harada, Y., and Asakura, T., 1996, "Radiation forces on a dielectric sphere in the Rayleigh scattering regime," J. Optics Communications, 124, pp. 529-54